Measuring Nanometer Displacements of Piezoelectric Transducers with an Optical Ruler

Intel Science Talent Search
Physics
November 2000

Christopher Wottawa

Kings Park High School
Kings Park, New York 11754

and

Laser Teaching Center
State University of New York at Stony Brook

Summary

In recent years, piezoelectric transducers (PZTs) have been developed with the ability to create nanometer displacements in response to an applied voltage. In this project, a Michelson interferometer was used as an 'optical ruler' to calculate the displacement factor of three separate PZT samples. The results showed an approximate movement of .632 nm/volt in the first two samples, and 1.149 nm/volt in the third sample.

Abstract

The use of specialized ceramic materials such as Lead Zirconium Titanate (PZT) to control motions on a nanometer scale has increased greatly in recent years. The purpose of this research was to measure the displacement factors (nanometers/volt) of a selection of PZT samples, at voltages up to 1000 V, using a Michelson Interferometer

In accordance with the Piezoelectric Effect, an applied voltage will cause a PZT to exhibit a tiny (typically nanometer) mechanical displacement, or vice versa. The applications of the Piezoelectric effect has reached almost every field of science and technology, being utilized in such advances as the atomic force microscope, any form of vibration suppression, and even the grill lighters used in a barbeque.

The displacements were measured using the beams of light from a He-Ne laser (wavelength = 632.8 nm) in a Michelson Interferometer to calculate the minute motions. After measuring the fringe shifts from the Michelson, the displacement factor for the first two samples were discovered to be approximately .632 nanometers for every volts, while the displacement factor of the third sample was calculated to about 1.149 nm/volt. With the ability to develop this method more efficiently, engineers will be able to test to the exact displacement factors of any PZT. They can then use this knowledge to apply exact voltages and produce nanometer displacements with an incredibly small margin of error. Knowing this is immensely important, especially in the ever-growing field of nano-technologies, where the smooth movements of a PZT would be able to move minute parts and manufacture tiny materials.

1 Introduction

With the current rise of nanotechnology and the ever increasing need for precise motion control in nearly every field of science and engineering, special ceramic materials with piezoelectric properties have grown tremendously in importance. These materials are referred to as PZTs, which is an abbreviation for both 'piezotransducer' and the most commonly used type of ceramic material, lead (plumbum) zirconium titanate.

PZTs have the capacity to sense structural faults in bridges, signs of failure on airplane wings, and monitor the integrity of skyscrapers. With these sensory systems integrated into a feedback loop along with piezoelectric actuators, the structures actually gain the ability to repair themselves [1,2,3]. Recently, PZTs have even been constructed into gossamer 30 micrometer thick fibers, to allow more efficient embedded smart structures [4].

In science applications, the PZT has led to the development of new cutting edge instruments that can actually measure surface topography on a scale from angstroms to 100 microns, counteracting minor variables such as fluctuations in the Earth's atmosphere, in a device called the Atomic Force Micropscope (AFM)[5].

The purpose of this research was to measure the displacement factors (nanometers/volt) of a selection of PZT samples, at voltages up to 1000 V, using a Michelson Interferometer. The interferometer was a assembled with the PZT mounted to the moveable mirror. The intensities of the central fringe in the interference rings – as a function of applied voltage – were recorded with a photodetector and used to calculate the displacements.

2 Piezoelectric Effect

The Piezoelectric Effect was discovered in 1880 by Pierre and Jacques Curie, as the property of certain crystals to generate an electrical charge when placed under mechanical pressures [6]. Likewise, when the PZT receives an applied voltage it produces a tiny displacement. Although most natural materials respond to this effect, the response is usually to such a small degree that piezoelectric applications using these materials are limited. Ferroelectric materials and polycrystalline ceramic materials, such as Barium Titanate (BT) and Lead Zirconium Titanate (PZT), magnify this effect to a usable standard. This is partially because of the isotropic structure of the materials. The centro-symmetric structure of a molecule of Lead Zirconium Titanate can be seen in Figure 1 below [7].

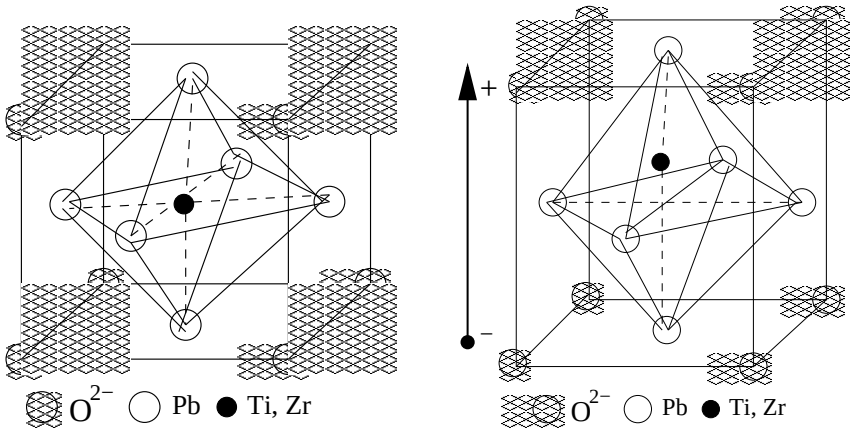

Figure 1: (Left)This is the structure of a molecule of Lead Zirconium Titanate before poling. (Right)This shows the resulting ansiotropic structure of the PZT after poling. Note the elongation of the PZT after it aquires a polarity. [7]

Dipoles with parallel orientation are scattered randomly throughout the PZT, prior to its applied voltage, in areas known as Weiss Domains. This electric dipole behavior is caused by the charge separation between the positive and negative ions. When an electric field is presented, the dipoles align, and the structure elongates parallel to the axis of the field. Likewise, the structure contracts perpendicular to the

field's axis. This process is depicted in Figure 2 below.

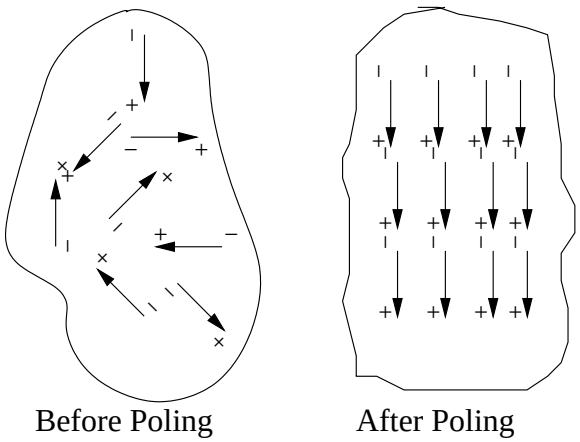

Figure 2: The Wiess Domains of a PZT material before and after poling [7].

After cooling, the Weiss Domains retain their polarity, as well as the resulting ansiotropic structure, as shown in Figure 1 on the previous page.

This process is repeatable. When an already poled PZT receives more voltage, the Weiss Domains shift in proportion to the new electric field, and the dimensions of the PZT change accordingly.

3 The Michelson Interferometer

Interferometry is an area of study that deals with the properties of interfering light. According to the law of superposition, when two beams of light interfere, the amplitude of the resulting beam is equal to the sum of the individual ampltudes of the two original beams. When two beams interfere, the phase difference – the variations of the resultant amplitudes as calculated by superposition – lead to alternating areas of constuctive and destructive interference, in what are commonly called interference fringes [8,9].

In the late 1880's A.A. Michelson set out to measure the length of a light wave. His device used two mirrors and a semi-transparent beamsplitter to cause two beams of light to interfere, creating the interference fringes. The reasoning behind the circular

shape of the fringes are described in detail in the Appendix found on the last two pages.

As used in this project, the Michelson can function as an optical ruler, measuring distances in wavelengths of light. It is the phase differences in the two sources which cause the appearance of fringes. In the Michelson interferometer, because coherent light is used, the phase shift is changed by manipulating the differences in the distances the beams must travel. By changing the distance of one beam, moving one of the mirrors foward or back, the phase shift is also changed, causing the places of constructive and destructive interference to change, giving the impression that the bullseye fringes are expanding inward or outward, depending on the movement of the mirror. The exact distance these fringes shift is directly related to the change in the path length.

The basic set-up of a Michelson interferometer is shown in Figure 3.

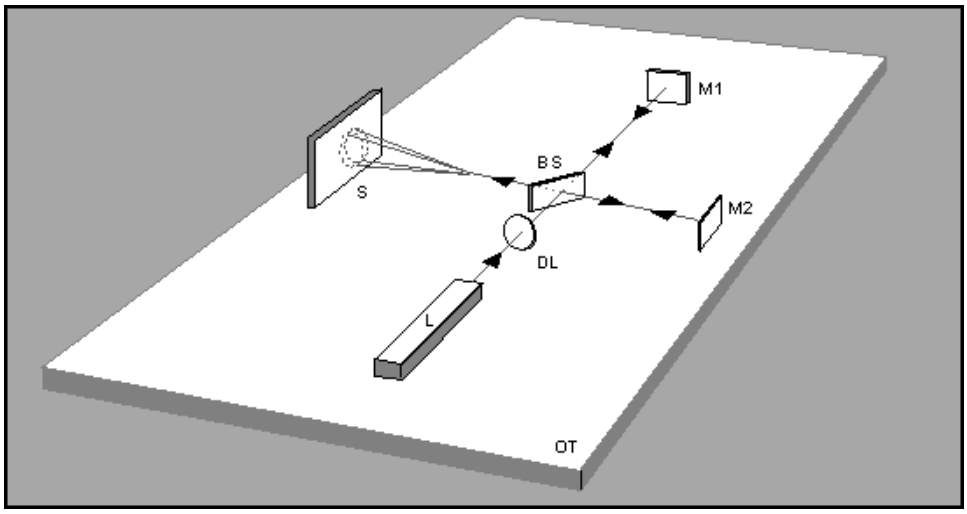

Figure 3: This shows the basic set-up of a Michelson Interferometer. The beam originates from the laser (L), diverges through the lens (DL) and strikes the beam splitter(BS). At this point the original beam splits into two perpendicular beams, one reflecting off mirror M1, the other reflecting off mirror M2. The beams are reflected back to the beam splitter, where they recombine and are projected towards the screen (S)[6]. (Image from `http://www.3dimagery.com/parttwo.html`)

4 Experimental Methods and Procedures

The construction of the experimental apparatus involved three major steps: 1– Arranging the laser, lenses and mirrors to create a laser beam of the correct size, divergence, and position; 2– assembling and aligning the interferometer itself and eliminating unwanted vibrations that initially made the fringes unstable; and 3– finding an efficient method for mounting the PZT behind the moveable interferometer mirror.

Initially the entire apparatus was mounted directly onto a large Newport optics table (5 ft × 8 ft). To achieve better vibration isolation, the interferometer portion was later transferred to a separate 18 in × 18 in × 2 in VERE honeycomb optical breadboard, which was placed onto a sheet of bubblewrap on top of the Newport table. After transferring the interferometer to this breadboard there were still too many vibrations to take any recordings. This was because the relatively heavy 7.5 cm × 5.0 cm × 0.25 cm beam splitter was mounted from the side, and hanging freely. Once the beam splitter was mounted from underneath, the fringes became quite stable.

Standard ThorLabs mounts were used in mounting the laser, both lenses, all four mirrors, beam splitter, and the photodetector. The lenses and photodetector also came from Thorlabs, while the first-surface mirrors came from Edmund Scientific.

4.1 Preparing the laser beam

The laser used was a small 1 mW HeNe type originally used in bar-code scanners and now available from surplus companies. The direction of the laser beam tended to drift during the first hour of warmup, but after this was sufficiently stable.

Mirror 1 was mounted 11.5 cm from the laser, angled approximately 45°, to reflect the beam 90 ° to its right. Mirror 2 was mounted 25.0 cm from Mirror 1, also angled 45°, but to reflect the beam 90 ° to its left. These two mirrors were used to easily adjust the angle and position of the beam when directing it into the interferometer.

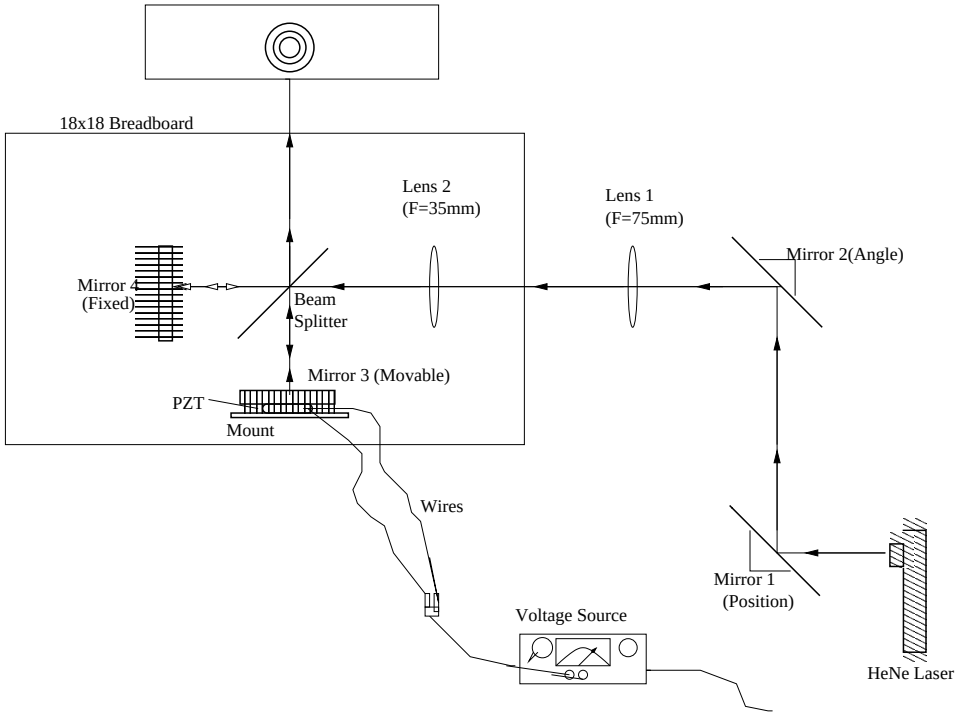

Figure 4: Final arrangement of the experimental apparatus

Next, a telescope was assembled using a lens with focal length (FL) 75 mm followed by one with 200 mm FL placed 275 mm further downstream. Since the separation between the two lenses was equal to the sum of their focal lengths, this arrangement expanded and collimated beam.

4.2 Constructing the interferometer

The interferometer was constructed using two first surface mirrors and a beam splitter. The beam splitter was positioned exactly 8.5 cm from the second lens, at a 45° angle. The fixed mirror was mounted 8.5 cm from the beam splitter. For the adjustable mirror, a second first surface mirror was mounted to a standard Thorlabs translating mount, with a micrometer screw, placing it approximately 9 cm from the beam splitter. The finished apparatus is shown above in Figure 4.

In order to create the pattern of interference, the mirrors had to be aligned perfectly, and cause the beams to interfere. As mentioned in Appendix A, in order for

circular fringes to be obtained, both mirrors in the interferometer had to be exactly perpendicular to the path travelled by the laser beams. During the experimentation, the mirrors were aligned in a specific order, and with a specific method. First, the angle mirror (2) was adjusted using the micrometer screws on the mount until the height and left/right positioning of the beam was constant. Next, the position mirror (1) was adjusted with the same procedure until the beam was projected to the exact center of both lenses. The lenses had to be exactly the same height, and same distance from right to left. First the position mirror would be adjusted to place the beam in the center of the first lens; then the angle mirror was adjusted to place the beam in the center of the second lens. This was repeated until the beam passed through both centers.

Next, before the beam splitter was set in place, mirror 4, the fixed mirror on the interferometer had to be aligned with the micrometer screw until the beam was reflected directly back to the source of the laser. Then the beam splitter could be set in place creating: the transmitted beam which still reflected from mirror 4 back to the laser; and the reflected beam. The beam splitter was angled until the reflected beam was exactly 90 ° from the transmitted beam. At this point, the last mirror was set into place, and adjusted until the reflection of both beams occupied the same space on the screen.

After the beams were precisely aligned, the second lens in the telescope with FL = 200 mm was replaced with one with FL = 35 mm, creating a diverging beam and a larger field. Instantly, circular fringes appeared on the screen. Therefore the beam must have a larger diameter and diverging, in order to obtain the necessary circular fringes. In this set-up, the resultant diameter of the beam at the viewing screen was approximately 10 cm, compared to 1 cm in the original trial.

4.3 Mounting the PZT

Three PZTs (All obtained from Physik Instrumente) were each attached to separate mirrors and mounts that could be interchanged easily into the micrometer slide in the position of mirror 3. The first sample was a PIC-140 disk with a diameter of 20 mm and a thickness of 1 mm. The second device was also a round disk, but was a PIC-141 sample with a diameter of 16mm, and a thickness of .5 mm. The last sample was also a PIC-141, but was a (15 mm x 12.5 mm x .83 mm) rectangular plate. The two faces of the all three PZTs were coated with a very thin silver film, which acted as electrodes to produce a uniform electric field inside the PZT.

The PZT disk was mounted behind the moveable mirror so that the mirror was supported entirely by the PZT and directly responded to its displacements. This was done using 5-minute epoxy after soldering wires on to the silver contacts.

During the preliminary testing of the apparatus, once the voltage was applied, it took several seconds for even the smallest change to occur in the fringes, and even this movement was very small. After several experiments, it was discovered that these problems were caused by the way the epoxy was originally applied to the PZT, which allowed some epoxy to overlap the sides of the sample. The transducer was actually forcing the epoxy to move along with it, which caused the hesitation in the effect as well as diminishing it.

In the final procedure, much finer wires were used (30 gauge stranded) and these were soldered more quickly on to the PZT, which was set on a block of aluminum as a heat sink. The wires were connected via BNC cables to the voltage supply. Next, a piece of 2 mm sheet metal was epoxied to the face of the mirror mount. A piece of the same material was cut to a size slightly smaller than the PZT, and then epoxied on top of the original piece of sheet metal. The PZT was then epoxied on top of this material, with another small piece of sheet metal glued to the top of it. Finally the first surface mirror was epoxied on top of this. The final PZT mount is illustrated in

Figure 5.

Once the PZT was mounted differently, with the epoxy between it and the sheet metal, the applied voltage caused the fringes to shift instantly. This final mounting procedure was repeated for the next two samples.

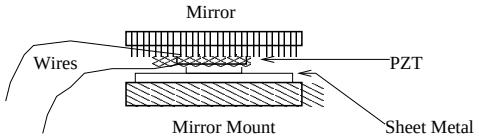

Figure 5: This shows the orientation of the PZT Mount

5 Measurements and Results

A photodetector was used to obtain accurate recordings of the intensity of the center of the fringe pattern. Therefore, low intensities correlated to periods of central destructive interference, and high intensities correlated to periods of central constructive interference.

The photo detector was positioned in the exact center of the fringes, at 0 volts. The voltage was then applied through increments of 10 volts, from 0 – 1000, with the photodetector measuring the resultant intensity of the beam. An intensity vs. voltage graph was then plotted in a spreadsheet program.

The results of the intensity vs. applied voltage measurement for the first sample can be seen in Figure 6 on the following page. At 0 volts the center fringe was a white spot, or an area of high constructive interference. That is why the first recordings appear as a peak on the graph. The changes in the intensity recorded into the photodetector (The points), which resulted from increased voltage, appear closely matched to the equation of a sine curve (The solid line). The crests of the curve are where the constructive interference was at its highest, and there was a white center, and the troughs are times of maximum central destructive interference, or a black center.

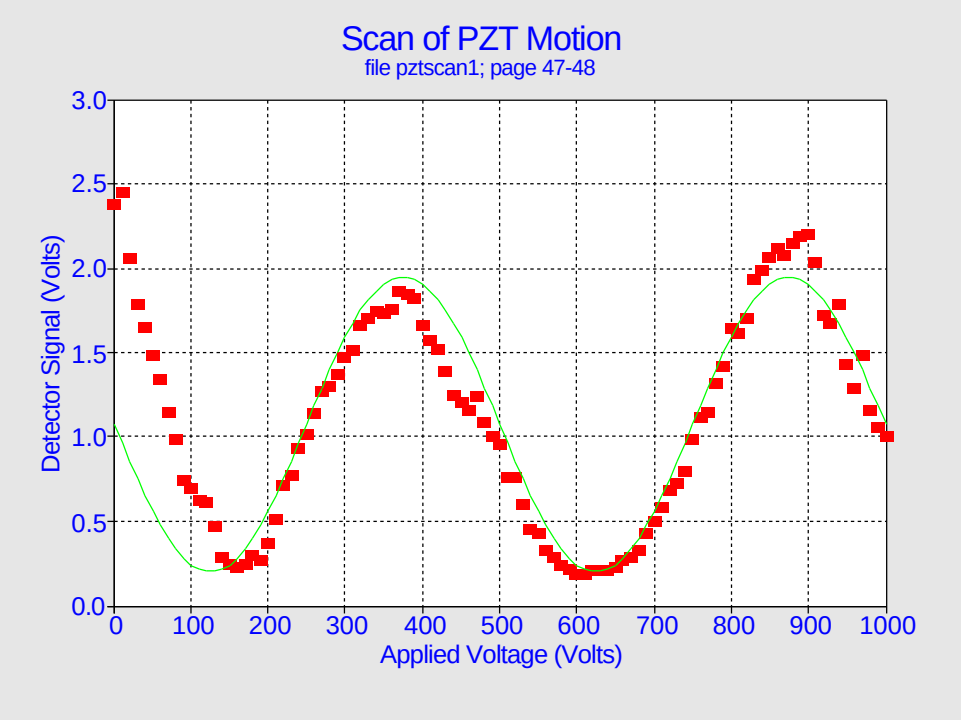

Figure 6: Measured light intensity at the photodector vs. applied voltage (points) for the first sample (PIC-140 with a diameter of 20 mm, and a thickness of 1.0 mm). The solid line is a sine curve that best matches the data. The period of this sine curve corresponds to the displacement factor.

5.1 Calculating the displacement factor for the first sample

Each wavelength of the sine curve in Figure 6 represents a full wavelength change in the path length, which means the PZT caused the mirror experienced a displacement of $\frac{\lambda}{2}$, . Therefore, the following equation was used to calculate the displacement factor(d) in nanometers per volt, where V_1 equals the voltage at the first crest, V_2 equals the voltage at the second crest and λ equals the wavelength of the laser beam.

$$d = \frac{\lambda}{2(V_2 - V_1)} \tag{1}$$

Inputting 632 nm for λ, 380 V for V_1, and 880 for V_2, the following equation was calculated.

$$d = \frac{632}{2(880 - 380)} \tag{2}$$

Resulting in a displacement factor of:

$$d = \frac{316nm}{500volts} \tag{3}$$

or .632 nm/volt.

5.2 Results and Displacement Factor of the Second Sample

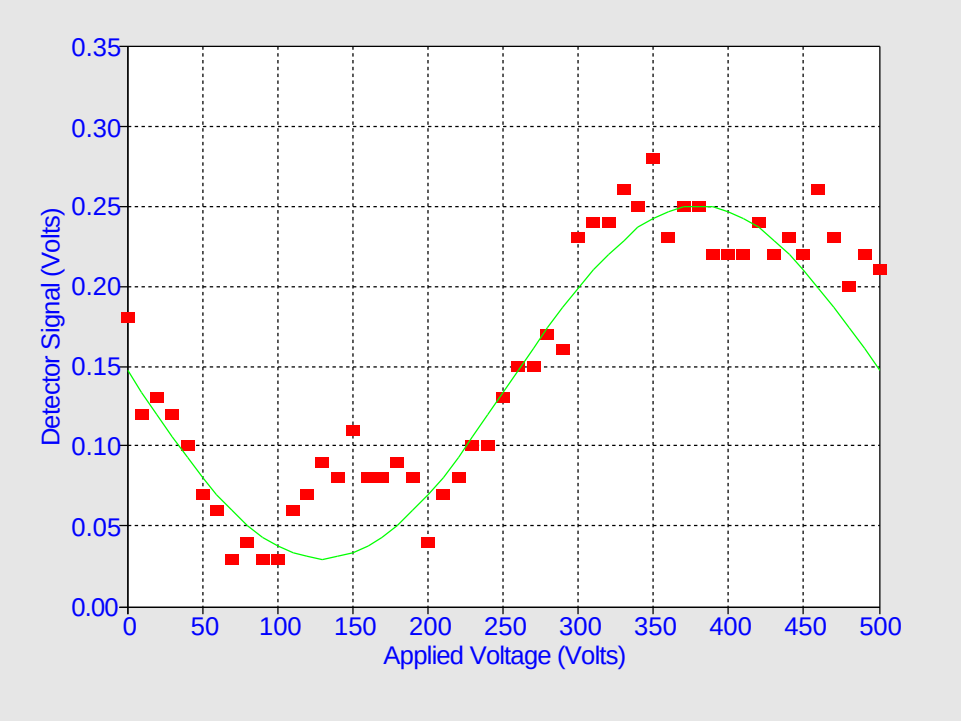

Figure 7: These are the results for the Second PZT (PIC-140, with diameter 16 mm, thickness, 0.5 mm.) Again, the solid line corrosponds to a sine curve that best matches the data.

The second PZT sample was mounted and tested in the same manner as the first sample, except its maximum voltage was 500 V (1000 V for every 1 mm diameter). Also, the first lens (FL = 75) was replaced with a different lens of the same size, but with a smaller focal length (FL = 35 mm). The second lens, (originally FL = 35)

was replaced with a lens with a focal length of 24.5 mm. This resulted in a greater divergance of the beam and a larger field. As seen on the results in figure 7, this set-up resulted in a lower range of detector signal intensities (.03 V to .29 V) compared to the first sample (.19 V to 2.45 V). Because of this lower range and the slight inaccuracies of the voltmeter, the results for the second PZT are not as accurate as the results from the first sample. Note the slight rise in the photo detector signal at 150 applied volts. The actual values are also farther from the best fit curve than in the results from the first sample, also due to the smaller range. These values do, however, fit the shape of a sine curve, and do depict a change from central constructive interference to central destructive interference. This means that the difference in path lengths of the two beams did change, and the PZT did exert its tiny displacement.

The displacement factor for this sample is calculated using the same equation as the first sample:

$$d = \frac{\lambda}{2(V_2 - V_1)} \tag{4}$$

Using 380 V for V_2 at the crest, and 130 V for V_1 at the trough (because there is only one crest in this graph) the original equation changes slightly. The denominator is doubled to compensate for only half the period being represented. Using 632 once again for λ, the equation becomes:

$$d = \frac{632}{4(380 - 130)} \tag{5}$$

This results in a displacement factor of:

$$d = \frac{316nm}{500volts} \tag{6}$$

or .632 nm/volt, which is equal to that of the first sample.

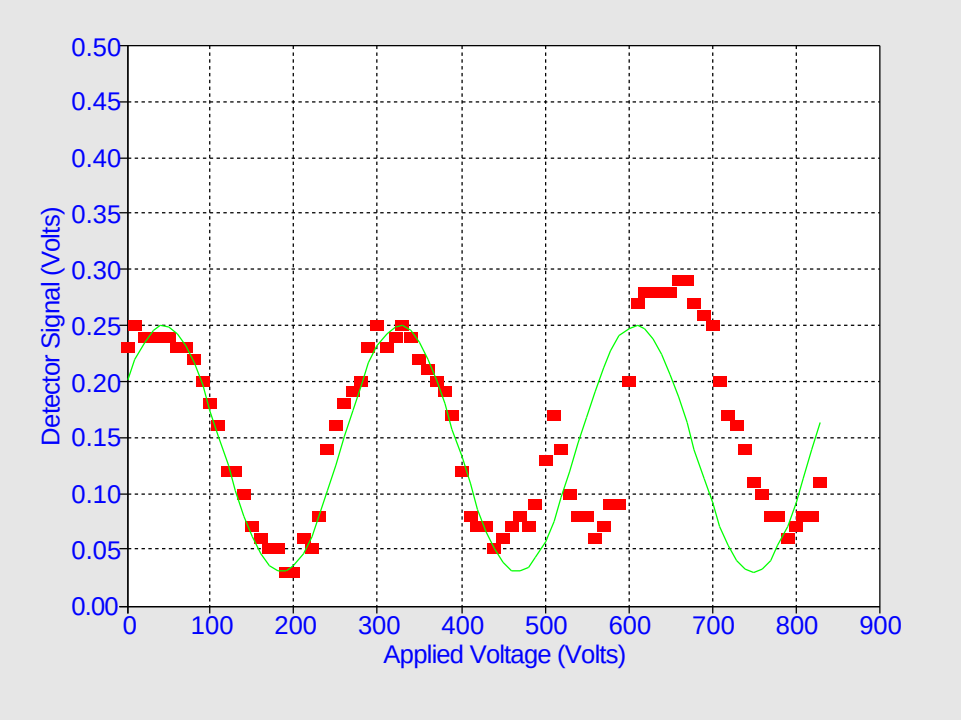

Figure 8: These are the results for the Third PZT (PIC-140, with dimensions: 15 mm x 12.5 mm x 0.83 mm)

5.3 Results and Displacement Factor of the Third Sample

The third sample, as mentioned before, was also a PIC-141, but was rectangular in shape and had a thickness of .83 mm (Maximum voltage = 830 V). This PZT was tested using the same lenses as the second sample, resulting in a greater divergance of the beams. The displacement factor of this PZT is again calculated with the same formula, placing 45 V for the value of V_1 at the first crest, and 325 for V_2 at the second crest. Using the same formula:

$$d = \frac{\lambda}{2(V_2 - V_1)} \tag{7}$$

$$d = \frac{632}{2(325 - 45)} \tag{8}$$

The displacement factor is calculated as:

$$d = \frac{316}{275} \tag{9}$$

or 1.149 nm/volt, almost twice that of the other two samples.

5.4 Summary of Results

The final results for the first three samples are shown in the following table. The first two PZTs were both recorded to have a displacement factor of .632, while the third had a displacement factor of 1.149.

Type	Thickness	Shape	Response Factor
PIC-140	1.00 mm	Disk	.632 nm/volt
PIC-141	0.50 mm	Disk	.632 nm/volt
PIC-141	0.83 mm	Plate	1.149 nm/volt

6 Discussion

Each set of results corrosponds to a sine curve. This is significant because the repeating series of crests and troughs represent repeating patterns of constructive and destructive interference – a property normally attributed to circular interference fringes. More importantly however, is the gradual change from the low points to high points, as the voltage increases. This represents a gradual change from a white center to a dark center, and the gradual change in the difference of path lengths of the two beams. This can only be attributed to the motion of the PZT. The period of the sine curve, according to previous calculations, shows that the the voltage is causing the piezoelectric material to expand .632 nanometers for every applied volt, or 1.149 in the case of the third sample.

Although this methodology provided an efficient way to measure displacements, more steps need to be taken to verify these recorded results. The first three mounted samples will be tested again with different lenses, creating a variance in the size of the resulting field and intensities of the fringes. With less divergance of the beams, the second and third PZTs may fit the respective sine curves more closely, or different discoveries will be made about the nature of PZTs, and how they function in different situations.

A mount will be constructed to provide for easy exchange of piezoelectric materials to a position behind the movable mirror. Then, PZTs of all shapes and sizes, disks and plates, with different thicknesses, and product types, specifically the PIC-155, PIC-150, and PIC-144 from Physik Instrumente will be tested, and compared to the original samples. With a system to automatically record the data, readings will be recorded faster and with more accuracy, with a 1 V integral at first (as opposed to 10 V) and then at fractions of a volt. With more samples, the specific property of PZTs that dictate the different displacement factors will be pinpointed.

Implementing the knowledge of the displacement factors, this research can take a multitude of various turns. A feedback loop can be created where a PZT sensor recieves pressure from a vibrating system and transfers it into a readable voltage. This voltage could be used through a series of amplifiers or resistors to create another voltage which would be input into another PZT, translated into a displacement that would counteract and dampen original vibrations. These PZTs can be embedded into a structure which is subjected to vibrations, acting as sensors or nerves. Knowing which devices are producing voltages and to what degree, the exact position and magnitude of the applied vibrations can be recorded.

7 Conclusion

Piezoelectric transducers effectively cause motions on an atomic scale without the slick-slip effect of friction. From this experiment, it was determined that a Michelson interferometer is an effective tool for measuring this movement. Although PZTs each have distinct properties which cause differences in displacement factors, each device has a constant rate of change. Therefore, it is possible to calibrated these nanometer motions to any set standard. Whether used in the construction of small machines or the sensing of unwanted pressures, this has the potential to reach a great variety of applications.

Literature Cited

1. Hogan, Hank. "Building with Brains." *Boy's Life* Jan 1998. Vol. 88, No. 1. pp.5(1)

2. Amato, Ivan. "Animating the Material World" *Science* Jan 17, 1992. Vol. 255, No. 5042. pp.284(3)

3. Williams, Gurney III. "Smart Materials" *Omni* April 1993. Vol. 15, No. 6. pp.42(6)

4. Wu, Corinna. "Smart Threads Act Sensitively when Hit." *Science News* August 1, 1998. Vol. 154, No. 5. pp.79(1)

5. AFM Imaging Technology Group "Atomic Force Microscope" `http://www.itg.uiuc.edu/ms/equipm`

6. Kistler Instrument Corporation. "The Piezoelectric Effect, Theory, Design, and Usage." `http://www.kistler.com/f_tech_theory_text.htm`

7. Physik Intrumente "Theory and Applications of Piezo Actuators and PZT NanoPositioning Systems" `http://www.physikinstrumente.com/tutorial/index.html`

8. Hecht, Eugene. *Optics: Third Edition.* Reading, MA: Addison-Wesley, 1998.

9. Ditchburn, R.W. *Light.* New York: Dover Publications, 1991.

10. 3D Imagery: "Producing Display Holograms Part II: Making Transmission and Reflection Holograms" `http://www.3dimagery.com/parttwo.html`

11. Tolansky, S. *An Introduction to Interferometry*, London and New York: Longmans, Green and Co., 1955

12. Davidson College, "Interference Fringes 101" `http://www.phy.davidson.edu/sethvc/Fringes/Pages/interference_pictures.htm`

Appendix: The Shape of the Interference Fringes

The geometric shape of the fringes can be explained using the following formulas derived from the conceptual image of the Michelson shown in Figure 9.

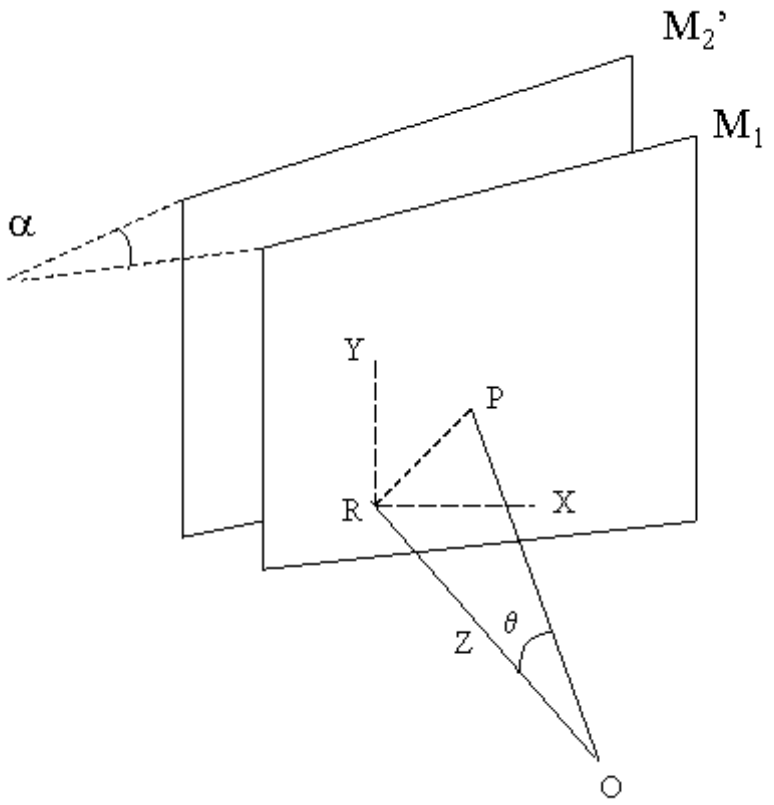

Figure 9: This image represents a theoritical view of the Michelson interferometer, used to get a mathematical view of the resulting interference fringes. (Image obtained from `http://www.phy.davidson.edu/sethvc/Fringes/Pages/interference_pictures.htm.`)

In the above diagram,M_1 and M_2 represent different planes, or the mirror surfaces of the Michelson interferometer. α is the angle between the planes. 0 is the perpective of the observer, with R at the base of the perpendicular. P is a point on M_1 on the (x, y) and z is the third axis. The first two formulas are derived from basic trigonometry, and geometry.

$$[OP]^2 = (x^2 + y^2 + z^2) \tag{10}$$

$$\cos\Theta = \frac{z}{\sqrt{x^2 + y^2 + z^2}} \tag{11}$$

The distance between the plates at R is equal to e, so the distance at P(d) falls into the following formula.

$$d = e + \tan\alpha \tag{12}$$

Constructive interference always occurs at:

$$n\lambda = 2d\cos\Theta \tag{13}$$

Substituting terms, the equation responsible for the shape of the fringes is as follows.:

$$n\lambda = \frac{2(e + \tan\alpha)z}{\sqrt{x^2 + y^2 + z^2}} \tag{14}$$

If the plates M_1 and M_2 were parallel and angle tan α was equal to 0, the following equation would result,

$$n\lambda = \frac{2ez}{\sqrt{x^2 + y^2 + z^2}} \tag{15}$$

which is equal to

$$x^2 + y^2 = \frac{4e^2}{n^2\lambda^2} - z^2 \tag{16}$$

the equation of a circle. Therefore, when the mirrors of the Michelson interferometer are exactly perpendicular, or the conceptual plates where the beams reflect are exactly parallel, the resulting fringes appear circular [11,12].

Summary

In recent years, piezoelectric transducers (PZTs) have been developed with the ability to create nanometer displacements in response to an applied voltage. In this project, a Michelson interferometer was used as an 'optical ruler' to calculate the displacement factor of three separate PZT samples. The results showed an approximate movement of .632 nm/volt in the first two samples, and 1.149 nm/volt in the third sample.